Shortcomings of the bond orientational order parameters for the analysis of disordered particulate matter

Walter Mickel, Sebastian Kapfer, Gerd Schröder-Turk, Klaus Mecke

AIP | The Journal of Chemical Physics

Shortcomings of the bond orientational order parameters for the analysis of disordered particulate matter

Walter Mickel, Sebastian C. Kapfer, Gerd E. Schröder-Turk, and Klaus Mecke

Citation: J. Chem. Phys. **138**, 044501 (2013); doi: 10.1063/1.4774084
View online: http://dx.doi.org/10.1063/1.4774084
View Table of Contents: http://jcp.aip.org/resource/1/JCPSA6/v138/i4
Published by the American Institute of Physics.

Shortcomings of the bond orientational order parameters for the analysis of disordered particulate matter

Walter Mickel,[1,2,3,a)] Sebastian C. Kapfer,[1,b)] Gerd E. Schröder-Turk,[1,c)] and Klaus Mecke[1,d)]

[1]*Theoretische Physik, Friedrich-Alexander-Universität Erlangen, Staudtstr. 7, D-91058 Erlangen, Germany*
[2]*Université de Lyon, F-69000, Lyon, France and CNRS, UMR5586, Laboratoire PMCN, Lyon, France*
[3]*Institute for Stochastics, Karlsruhe Institute of Technology, D-76128 Karlsruhe, Germany*

(Received 28 September 2012; accepted 13 December 2012; published online 22 January 2013)

Local structure characterization with the bond-orientational order parameters q_4, q_6, ... introduced by Steinhardt *et al.* [Phys. Rev. B **28**, 784 (1983)] has become a standard tool in condensed matter physics, with applications including glass, jamming, melting or crystallization transitions, and cluster formation. Here, we discuss two fundamental flaws in the definition of these parameters that significantly affect their interpretation for studies of disordered systems, and offer a remedy. First, the definition of the bond-orientational order parameters considers the geometrical arrangement of a set of nearest neighboring (NN) spheres, NN(p), around a given central particle p; we show that the choice of neighborhood definition can have a bigger influence on both the numerical values and qualitative trend of q_l than a change of the physical parameters, such as packing fraction. Second, the discrete nature of neighborhood implies that NN(p) is not a continuous function of the particle coordinates; this discontinuity, inherited by q_l, leads to a lack of robustness of the q_l as structure metrics. Both issues can be avoided by a morphometric approach leading to the robust *Minkowski structure metrics* q_l'. These q_l' are of a similar mathematical form as the conventional bond-orientational order parameters and are mathematically equivalent to the recently introduced Minkowski tensors [G. E. Schröder-Turk *et al.*, Europhys. Lett. **90**, 34001 (2010); S. Kapfer *et al.*, Phys. Rev. E **85**, 030301(R) (2012)]. © *2013 American Institute of Physics*. [http://dx.doi.org/10.1063/1.4774084]

In 1983, Steinhardt *et al.*[1] proposed the family of local q_l and global Q_l bond-orientational order (BOO) parameters as a three-dimensional generalization of the ψ_6 hexatic order parameter in two dimensions.[2] Bond orientation analysis has become the most commonly used tool for the identification of different crystalline phases and clusters, notably fcc, hcp, and bcc,[3–9] or icosahedral nuclei.[10–12] They are also used to study melting transitions[10,13,14] and interfaces in colloidal fluids and crystals.[15] For the study of glasses and super-cooled fluids, q_6 and Q_6 have become the most prominent order parameters when searching for glass transitions[16–19] and crystalline clusters.[4,8,11,20–22] While q_l is defined as a local parameter for each particle, other studies have used global averages of bond angles (Q_l) to detect single-crystalline order across the entire sample.[23–25]

The BOO parameters q_l and Q_l are defined as structure metrics for ensembles of N spherical particles. For a given sphere a, one assigns a set of nearest neighbors (NN) spheres NN(a). The number of NN assigned to a is $n(a) = |\mathrm{NN}(a)|$. Any two spheres a and b are said to be connected by a *bond* if they are neighbors, i.e., if $a \in \mathrm{NN}(b)$.[26] The set of all bonds is called the *bond network*. The idea of bond orientation analysis is to derive scalar metrics from the information of the bond network (i.e., the set of bond vectors). The precise definition of the bond network is therefore crucial.

For a sphere a, the set of unit vectors $\mathbf{n}_{ab}$ points from a to the spheres $b \in \mathrm{NN}(a)$ in the neighborhood of a. Each vector $\mathbf{n}_{ab}$ is characterized by its angles in spherical coordinates θ_{ab} and φ_{ab} on the unit sphere. Following Steinhardt *et al.*,[1] the local BOO $q_l(a)$ of *weight* l assigned to sphere a is defined as

$$q_l(a) = \sqrt{\frac{4\pi}{2l+1}\sum_{m=-l}^{l}\left|\frac{1}{n(a)}\sum_{b\in\mathrm{NN}(a)} Y_{lm}(\theta_{ab},\varphi_{ab})\right|^2}, \quad (1)$$

where Y_{lm} are spherical harmonics (see, e.g., Appendix in Ref. 31). This formula can be interpreted as the lowest-order rotation-invariant (that is, independent of the coordinate system in which θ_{ab} and φ_{ab} are measured) of the lth moment in a multipole expansion of the bond vector distribution $\rho_{\mathrm{bond}}(\mathbf{n})$ on a unit sphere. Higher-order invariants, often termed w_l, are defined in a similar way.[1,32,33]

There are other structure metrics derived from the bond network, such as centro-symmetry metrics,[27] Edwards configurational tensor,[28] fcc/hcp-order metrics,[29] or the number of bonds as the most simple topological characteristic,[30] but the Steinhardt bond orientational order parameters are most commonly used.

The existence of spheres with values of q_4 and q_6 close to those of an ideal ordered structure (see Table I) has been

a)Electronic mail: waltermickel@web.de.
b)Electronic mail: kapfer@ens.fr.
c)Electronic mail: Gerd.Schroeder-Turk@physik.fau.de.
d)Electronic mail: Klaus.Mecke@physik.fau.de.

interpreted as evidence of ordered clusters. The local structure metrics q_l have been used to identify fcc, hcp, bcc or icosahedral structures in condensed matter and plasma physics (e.g., in colloidal particle systems,[4] random sphere packings,[23,34] or plasmas[35]) by analyzing histograms over the (q_4, q_6)-plane or combinations of similar order parameters.[6] Frequently, histograms of one order parameter only, namely, q_6, are used to qualitatively compare disorder in particulate matter systems.[5,20,36,37] Our previous work[38] has raised the caution that local configurations can exist that are clearly non-crystalline but have the same values of q_6 as hcp or fcc environments. Several authors have defined bond order functions[39] closely related to the q_l for the identification of crystalline clusters.[11,15,21,40]

As a different application from the identification of locally crystalline domains, it has been proposed to use averages $\langle q_l \rangle$ over all spheres to quantify the degree of order of a configuration. Averages $\langle q_6 \rangle$ have been analyzed (as functions of some control parameters such as temperature, pressure, strain, or packing fraction) for random sphere packings,[20] granular packing experiments,[41] model fluids,[42] molecular dynamics simulations of water,[43] or polymer melts.[44] This use of $\langle q_l \rangle$ to quantify the overall degree of order implies a monotonous relationship between the value of q_l and the degree of order. In contrast to the identification of individual crystalline cells as those with q_l the same as for the crystalline reference cell q_l^{cryst}, one now assumes that larger values of $\Delta := |q_l - q_l^{\mathrm{cryst}}|$ correspond to "larger" deviations from the crystalline configuration, even for clearly acrystalline local configurations with large values of Δ. The validity of this assumption is difficult to assert, in the absence of an independent definition of the degree of the "deviation from crystalline structure." (Note also the obvious problem for the case of monodisperse hard spheres, where two distinct crystal reference states, fcc and hcp, exist, which however have different values of q_l.) Nevertheless, q_6 has been used to quantify order in disordered packings, under the assumption that higher values of q_6 correspond to higher degree of order.[45] Unless the system represents a small perturbation of one specific crystalline state, this use of q_6 is, in our opinion, not justified. q_6 is not a suitable order metric to compare the degree of order of disordered configurations that are far away from a crystalline reference state. We use the term *structure metric* to emphasize that *a priori* q_l does not quantify order in disordered systems.

We here demonstrate a further aspect, distinct to those described above, that should be taken into account when interpreting q_l data for disordered systems, namely, a very significant dependence of the q_l values on details of the definition of the bond network: changes of the NN definition do not only affect the absolute values (which are of great importance, as the comparison to the crystalline reference values is in terms of these absolute values) but they can also affect functional trends. This observation highlights the problem in the interpretation of anomalies of the BOO parameters (that is, local extrema as function of some thermodynamic parameter) as being connected to thermodynamic anomalies;[42,43] see also the discussion of the anomalies of water[46] in terms of a parameter similar to the BOO parameters. Rather than being a mere inconvenience, the dependence on the details of the bond network definition is of direct relevance to the physical interpretation.

AMBIGUITY OF THE NEIGHBORHOOD DEFINITION AND ITS EFFECT ON q_l

The choice of a set of nearest neighbors—at the heart of bond orientation analysis—is not unique (see Fig. 1). Steinhardt *et al.*[1] proposed to use "some suitable set" of bonds for the computation of q_l; they used a definition based on a cutoff radius of 1.2σ, where σ is the particle diameter.[1] That is, each sphere that is closer to a given sphere a than a cutoff radius r_c is assigned as a NN of sphere a. Neighborhood definitions based on cutoff radii are widely used, e.g., with cutoff radii 1.2σ and 1.4σ[11,18,24,37,47] or with the value of the cutoff radius determined by the first minimum of the two-point correlation function $g(r)$.[9,14,15,25,48]

Alternatively, the Delaunay graph of the particle centers[49,50] is used to define NN.[5,20,23,41,51] In this parameter-free method, every sphere which is connected to a sphere a by a Delaunay edge is considered a NN of a. A rarely used definition is to assign a fixed number n_f of NN to each particle, $n(a) = n_f$.[42,43] In three dimensions, the $n_f = 12$ other spheres closest to the central sphere are chosen as neighbors. The difference between these definitions is illustrated in Fig. 1. Note that while the definitions via cutoff radius and via the Delaunay graph are symmetric, i.e., $b \in \mathrm{NN}(a) \Leftrightarrow a \in \mathrm{NN}(b)$, the definition of neighborhood as the nearest n_f spheres is not, see Fig. 1(d). The definitions of NN discussed so far will be called *bond network neighborhoods* in the following; in this picture, each nearest neighbor is equivalent to the other neighbors. By contrast, we use the term *morphometric neighborhood* if the

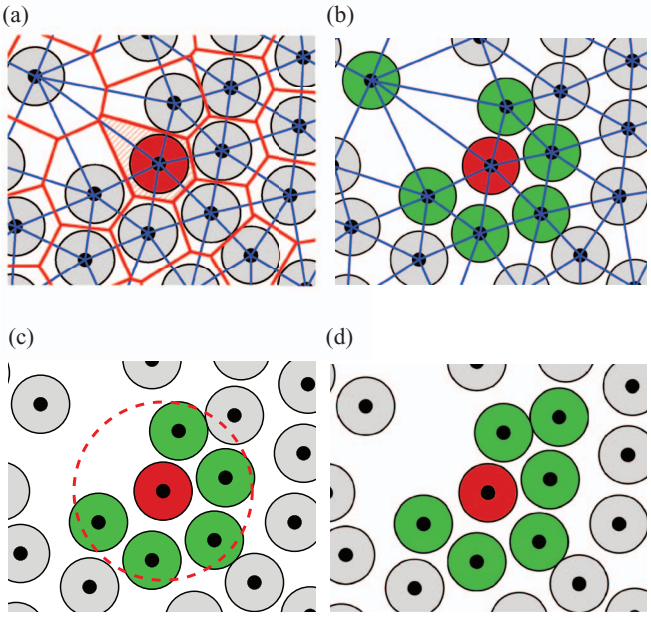

FIG. 1. Widely used NN definitions: (a) Voronoi diagram (red) and its dual, the Delaunay graph (blue). (b) Delaunay definition of nearest neighbors (NN): the Delaunay neighbors of the red sphere are highlighted in green. (c) NN definition with cutoff radius r_c. (d) n_f closest NN, here $n_f = 6$.

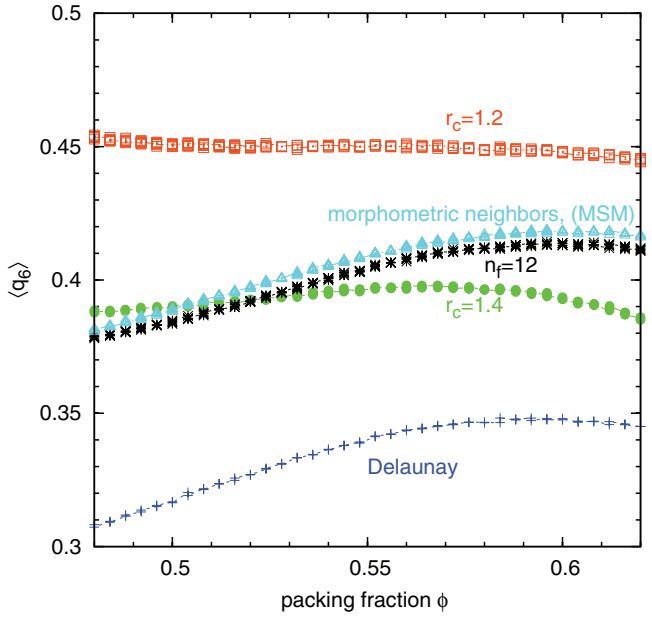

FIG. 2. Average local bond order parameter $\langle q_6 \rangle$ in the super-cooled HS fluid with several definitions of the nearest neighbors: orange squares: $r_c = 1.2\sigma$, green bullets: $r_c = 1.4\sigma$, blue crosses: Delaunay definition, and black stars: $n_f = 12$. The turquoise triangles represent data for the Minkowski structure metrics (MSM) $\langle q_6' \rangle$ defined in Eq. (2).

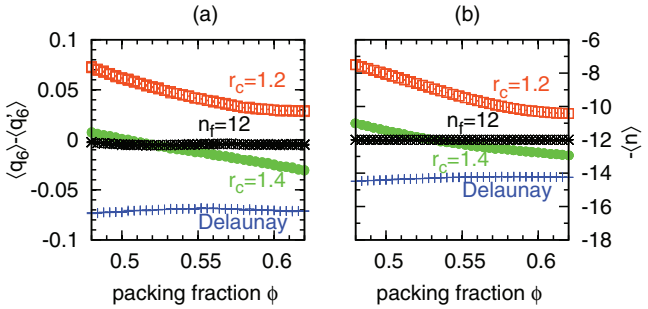

FIG. 3. (a) Average number of nearest neighbors identified by the different definitions of neighborhood, for the same data as shown in Fig. 2. Difference $\langle q_6^X \rangle - \langle q_6' \rangle$ between q_6 values for different definitions of the bond network neighborhood, $X = \{r_c = 1.2\sigma, r_c = 1.4\sigma, \mathrm{D}, n_f = 12\}$. (b) Comparison of the functional trend of these data to $-\langle n \rangle(\phi)$ demonstrates the strong negative correlation of the value of q_6 with the number of NN spheres n identified by the specific neighborhood definition.

neighborhood relation is additionally weighted with geometrical features.

A principal weakness of structure metrics based on bond network neighborhoods is their lack of robustness: Small changes of particle positions can delete or add entries in the set of neighbors. This discontinuity with respect to the particle positions is inherited by the structure metrics defined via bond network neighborhoods. Small changes in the particle coordinates can lead to large changes in the structure metrics, which is undesirable.

We demonstrate the very strong effect of the NN definition on the BOO parameter q_6 by the example of a super-cooled fluid. Using non-equilibrium molecular dynamics (MD) simulations,[52–54] super-cooled configurations are generated that represent entirely disordered states with densities larger than the fluid-crystal coexistence density of hard spheres (HS) of $\phi \approx 0.494$.[55]

Figure 2 shows the average local BOO $\langle q_6 \rangle$ for four different choices of bond network neighborhood definition. To distinguish between the different definitions of neighborhood discussed above, we use the symbols $q_6^{r_c}$, q_6^{D}, and $q_6^{n_f}$. First, the absolute values of $q_6^{r_c=1.2\sigma}$, $q_6^{r_c=1.4\sigma}$, $q_6^{n_f=12}$, and q_6^{D} differ significantly, which is important when comparing these values to that of a specific crystalline phase such as fcc. Second, and of greater concern for the use of q_6 as a structure metric, the behavior of $q_6^{r_c=1.2\sigma}$, $q_6^{r_c=1.4\sigma}$, $q_6^{n_f=12}$, and q_6^{D} is qualitatively different as a function of the packing fraction ϕ. For example, $\langle q_6^{r_c=1.2\sigma} \rangle(\phi)$ shows a slight negative trend without pronounced extrema, whilst $\langle q_6^{r_c=1.4\sigma} \rangle(\phi)$ increases for $\phi < 0.56$ and decreases above. $\langle q_6^{n_f=12} \rangle(\phi)$ and $\langle q_6^{\mathrm{D}} \rangle(\phi)$ show a maximum at slightly different positions with a significantly different absolute value. Each of these trends is specific to the neighborhood definition. These discrepancies raise a caution flag about the use of q_6 as a local structure metric in disordered systems. This is in accordance with several reported difficulties in the application of q_6 in ordered and disordered systems.[45,56,57] The choice of the NN definition has a dominant effect on the values and on the functional trend of $\langle q_6 \rangle(\phi)$ that conceals the behavior due to genuine structural changes induced by the physics of the system. Results for q_6 obtained by different studies are not only difficult to compare quantitatively, but also the qualitative behavior may be misleading.

The behavior of $\langle q_6 \rangle$ can be rationalized by considering the average number of nearest neighbor spheres $\langle n \rangle(\phi)$ identified by the different neighborhood definitions.

Figure 3(a) shows $\langle q_6 \rangle - \langle q_6' \rangle$ as function of ϕ. q_6' is a structure metric based on morphometric neighborhood, which is discussed in detail in the section "Minkowski structure metric by Voronoi-cell weighting". Figure 3(b) shows $-\langle n \rangle$. These data demonstrate a very close correlation between $\langle q_6 \rangle - \langle q_6' \rangle$ and $-\langle n \rangle$, valid for all neighborhood definitions. This result asserts that $\langle q_6' \rangle$ captures physical structure properties, while various variants of $\langle q_6 \rangle$ are predominantly indicative of the typical number of NN spheres $\langle n \rangle$ identified by the respective NN definitions.

Figure 4 further corroborates this observation by the analysis of $\langle q_6^{n_f=n} \rangle$ as a function of n for the super-cooled hard sphere fluid at $\phi = 0.600$. The average $\langle q_6^{n_f=n} \rangle(n)$ systematically decreases with higher prescribed numbers n_f of NN. This effect is further amplified for large $n_f > 12$, when spheres in the second coordination shell are also identified as neighbors. The stronger decrease in q_6 when encountering the second coordination shell also explains why $\langle q_6^{\mathrm{D}} \rangle$ generally has lower values compared to the other neighborhood definitions, since the typical number of Delaunay neighbors is higher than for the other neighborhood definitions, $\langle n_a^{\mathrm{D}} \rangle \approx 14$.

MINKOWSKI STRUCTURE METRIC BY VORONOI-CELL WEIGHTING

This section introduces the Minkowski structure metrics (MSM) q_l' that were already alluded to above. The Minkowski

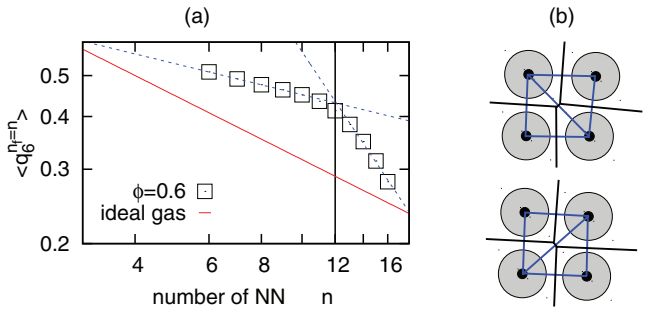

FIG. 4. (a) Mean $\langle q_6^{n_f=n}\rangle$ as a function of the fixed number n of neighbors assigned to each sphere. The squares are data of a super-cooled fluid with $\phi = 0.6$ and the red solid line of the ideal gas ($\langle q_6^{n_f=n}\rangle \propto n^{-1/2}$, see Ref. 58). The dotted lines are fits for the first coordination shell for $n < 12$, and first and second shell $n > 12$. The first shell exponent is -0.24 and the second shell exponent is -1.48. (b) Illustration for the discontinuity of the topology of the Voronoi diagram as function of center point coordinates: An infinitesimal particle displacement can destroy or create Voronoi cell facets (and hence bonds in the neighborhood definition based on the Delaunay graph).

structure metrics are obtained by an adaption of the conventional BOO parameters. The MSM differ from the conventional q_l, Eq. (1), by the fact that the contribution of each neighbor to the structure metric is weighted by an associated relative area factor $A(f)/A$. In this factor, $A(f)$ is the surface area of the Voronoi cell facet f separating the two neighboring spheres that correspond to a given bond, and $A = \sum_{f\in\mathcal{F}(a)} A(f)$ is the total surface area of the Voronoi cell boundary $\mathcal{F}(a)$ of sphere a. This simple change leads to robust, continuous, and parameter-free structure metrics q_l' that avoid the shortcomings of the conventional q_l discussed above. (Note also the similar suggestion by Steinhardt *et al.*[1] to weigh Delaunay edges by the solid angle subtended by the corresponding Voronoi facet.)

We define

$$q_l'(a) = \sqrt{\frac{4\pi}{2l+1}\sum_{m=-l}^{l}\left|\sum_{f\in\mathcal{F}(a)}\frac{A(f)}{A}Y_{lm}(\theta_f,\varphi_f)\right|^2}, \qquad (2)$$

where θ_f and φ_f are the spherical angles of the outer normal vector $\mathbf{n}_f$ of facet f. Note that the direction of this vector coincides with the bond vector that is used in conventional bond orientation analysis (see Fig. 1).

Because of the weighting of each bond by its corresponding Voronoi facet area $A(f)/A$, these newly constructed structure metrics q_l' are continuous functions of the spheres' center point coordinates, and hence robust. Furthermore, this geometrical neighborhood is symmetric and parameter-free.

The definition of q_l' results naturally from a multipole expansion in spherical harmonics of the Voronoi cell surface normal distribution function,

$$\rho(\mathbf{n}) = \frac{1}{A}\cdot\sum_{f\in\mathcal{F}}\delta(\mathbf{n}(f)-\mathbf{n})A(f), \qquad (3)$$

on the unit sphere: $\rho(\mathbf{n}) = \rho(\theta,\varphi) = \sum_{l=0}^{\infty}\sum_{m=-l}^{l} q_{lm}' Y_{lm}(\theta,\varphi)$, where q_{lm}' evaluates to $\sum_{f\in\mathcal{F}(a)}(A(f)/A)Y_{lm}^*(\theta_f,\varphi_f)$; the asterisk (*) denoting complex conjugation.

TABLE I. Values of q_l in perfectly symmetric configurations. For these highly symmetric cases (fcc, hcp, icosahedron, sc), all the definitions of neighborhood discussed in this article yield the same crystallographic neighbors, and hence, values of q_l (assuming infinite precision for the point coordinates such that the Delaunay diagram has edges to *all* nearest crystallographic neighbors). Spheres in bcc configuration have 8 nearest neighbors at distance σ, where σ is the particle diameter, and 6 second nearest neighbors at distance $\sqrt{2}\sigma$ have 14 Delaunay neighbors. n is the number of nearest neighbors.

	bcc $Im\bar{3}m$		fcc $Fm\bar{3}m$	hcp $P6_3/mmc$	Icosahedral	Simple cubic $Pm\bar{3}m$
	$n=8$	$n=14$	$n=12$	$n=12$	$n=12$	$n=6$
q_2	0	0	0	0	0	0
q_3	0	0	0	0.076	0	0
q_4	0.509	0.036	0.190	0.097	0	0.764
q_5	0	0	0	0.252	0	0
q_6	0.629	0.511	0.575	0.484	0.663	0.354
q_7	0	0	0	0.311	0	0
q_8	0.213	0.429	0.404	0.317	0	0.718
q_9	0	0	0	0.138	0	0
q_{10}	0.650	0.195	0.013	0.010	0.363	0.411
q_{11}	0	0	0	0.123	0	0
q_{12}	0.415	0.405	0.600	0.565	0.585	0.696

By contrast, the l-th moment of the distribution $\rho(\mathbf{n})$ in Cartesian coordinates is

$$W_1^{0,l} := \sum_{f\in\mathcal{F}}\underbrace{\mathbf{n}(f)\otimes\ldots\otimes\mathbf{n}(f)}_{l\text{ times}}A(f), \qquad (4)$$

where $\otimes$ denotes the tensor product. The moment tensors $W_1^{0,l}$ are special types of Minkowski tensors.[53,59] These versatile shape metrics have been studied in the field of integral geometry[60] and successfully applied to analyze structure in jammed bead packs,[38,61] bi-phasic assemblies,[62,63] foams,[64] and other cellular structures.[59,64] There is a one-to-one correspondence between this class of Minkowski tensors and the multipole expansion of the surface normal vector distribution $\rho(\mathbf{n})$ of a convex Voronoi polytope $\mathcal{F}(a)$.[65,66]

For ideal crystals where all Voronoi facets have equal size, the values of the BOO q_l and of the MSM q_l' are the same; these symmetries are fcc, hcp, the icosahedron, and sc (simple cubic). In the case of bcc, where Voronoi cells have in total 14 facets, of which 8 correspond to closest neighbors and 6 to neighbors in the second shell, q_l differ from q_l' (see also Table I).

The construction of the weighted q_l' has no adjustable parameters. However, the choice of the Voronoi diagram as the partition that defines local neighborhood and that is used for the definition of q_l' may be viewed as arbitrary. Its use can be justified as follows: First, the use of any partition of space into cells associated with the beads for the neighborhood definition guarantees symmetric neighborhoods, $(a\in\mathrm{NN}(b))\Leftrightarrow(b\in\mathrm{NN}(a))$. Second, the use of the Voronoi diagram ensures that the following minimal requirements are met: (a) convex cells, (b) invariance under exchange of spheres decorating the seed points, and (c) the possibility to reconstruct the seed point coordinates uniquely from the facet information.[67] The authors

are unaware of an alternative to the Voronoi diagram that fulfills these requirements.

GEOMETRIC INTERPRETATION OF THE MINKOWSKI STRUCTURE METRICS, IN PARTICULAR OF q_2'

For the use of both BOO parameters and MSM, an important issue is the choice of the weights l that are considered. Many studies restrict themselves to only q_6, possibly supplemented by q_4 and the associated higher-order invariants w_4 and w_6. This is likely to be motivated by q_6 being the apparent generalization of the two-dimensional hexatic order parameter ψ_6. The relation between the $l = 6$ structure metrics and ordering, however, is not as direct in 3D as it is in 2D: q_6 is maximized by icosahedral bond order, which is incompatible with translational order. The perception that large values of certain structure metrics, in particular q_6, are intrinsically connected with crystallization is therefore deceiving, and it is useful to discuss the relevance of the individual weights to physical problems.

In all cases, q_0' is trivially 1, while q_1' trivially vanishes due to the so-called *envelope theorems* of Müller[68] (note, this does not apply to q_1). Thus, the first weight that captures pertinent information about a disordered system is $l = 2$; for hcp and fcc crystals, q_2' vanishes. The invariants q_3' and q_5' (and odd weights in general) vanish in configurations symmetric under inversion, but capture deviations from this symmetry (see Table I). Hence, they might be robust candidates for defect detection like centro-symmetry metrics[27] or to separate hcp from fcc, since the hcp Voronoi cell is not inversion symmetric (see Table I), while fcc is inversion symmetric ($m\bar{3}m$) with respect to the sphere centers. Including Steinhardt *et al.*'s original paper[1] we are not aware of any applications of odd weights l. The lowest weight to discriminate a sphere from a cube is $l = 4$, and thus, plays an important role in ordered materials. The cubic-symmetry fcc, bcc, and simple cubic lattices all have non-vanishing q_4' values (for the conventional BOO parameters though, great care is needed for the bond definition, as different sets of NN for bcc reveal a dramatic change on conventional q_4). q_6 is the first non-vanishing weight for icosahedral symmetry (and adopts its maximal value for the regular icosahedron). Note that the q_6 values for fcc can be matched by deformed icosahedral bonds.

While in ordered states, the q_l are easily interpreted, in disordered states the lack of a well-defined reference state renders the interpretation more difficult. Figure 5 shows $\langle q_2' \rangle$, $\langle q_4' \rangle$, and $\langle q_6' \rangle$ of hard-sphere systems in a wide range of packing fractions. The plot includes data from Monte Carlo (MC) simulations of the thermal equilibrium fluid/solid,[53] from fully disordered and partially crystalline jammed Lubachevsky-Stillinger (jLS),[61,69] and also from unjammed non-equilibrium simulations (uLS) from LS simulations before jamming,[70] and the data from Fig. 2 (Matsumoto algorithm (MA-MD)).[52]

Empirically, we find that disordered cells virtually always have finite q_2' values; for order (cubic-symmetry or close packed), q_2' vanishes. Therefore, distributions of q_2' in a partially ordered system are bimodal, which is convenient for the separation of both phases. Conversely, if the abundance of small values $q_2' \approx 0$ in a sample vanishes, one can conclude that it is fully disordered. The information contained in the lowest weight q_2' is also captured in the anisotropy index $\beta_1^{0,2}$ derived from Minkowski tensors,[72] see the comparison of $\langle q_2' \rangle$ and $1 - \langle \beta_1^{0,2} \rangle$ in Fig. 5. The observation that q_2' vanishes for ordered configurations corresponds to the fact that $\beta_1^{0,2} = 1$, and $q_2' > 0$ corresponds to $\beta_1^{0,2} < 1$ (cf. Refs. 38, 53, and 61).

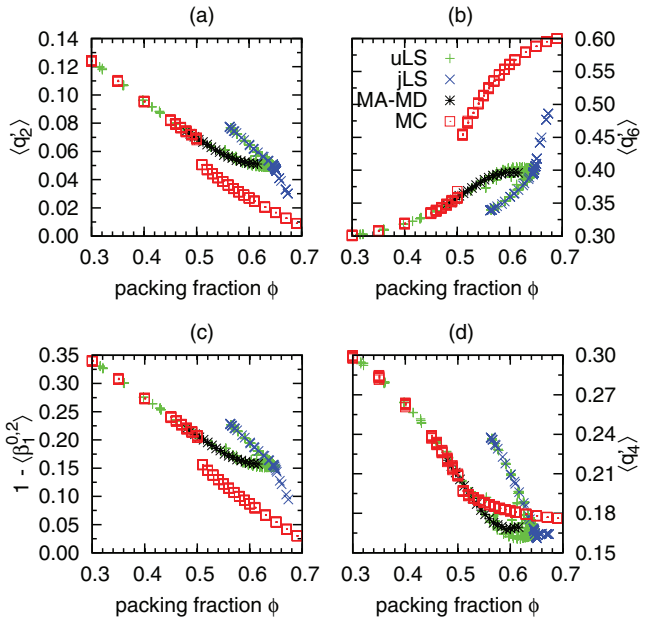

FIG. 5. Minkowski structure metrics q_2', q_4', and q_6' for equilibrium hard spheres Monte Carlo (MC)[53] simulations, jammed Lubachevsky-Stillinger (jLS),[61] non-equilibrium unjammed Lubachevsky-Stillinger (uLS),[71] and non-equilibrium Matsumoto algorithm (MA-MD) simulations;[52] (see text). $\beta_1^{0,2}$ is the anisotropy index, i.e., the ratio of the smallest and the largest eigenvalue of the Minkowski tensor $W_1^{0,2}$; see Eq. (4) and Ref. 61.

Both structure metrics, q_2' and $\beta_1^{0,2}$, capture well the different features in local structure of hard-sphere systems (Fig. 5, panels (a) and (c)). The thermodynamic phase transition from the fluid to the solid (fcc) phase at packing fractions around $\phi \approx 0.49$ is clearly visible. Furthermore, jammed sphere packs are well distinguished from the equilibrium configurations. Starting from the equilibrium and avoiding crystallization, the non-equilibrium MA-MD protocol continues the fluid branch into a super-cooled fluid regime. The uLS protocol generates further non-equilibrium states with larger q_2', up to jammed configurations. In both diagrams, (a) and (c), the non-equilibrium fluid states are found above the linear extrapolation of the equilibrium fluid branch, while the ordered phase is below. The diagram (b), showing $\langle q_6' \rangle$, reproduces (though "upside down") quite well the qualitative features obtained from $\langle q_2' \rangle$ or $\langle 1 - \beta_1^{0,2} \rangle$. The agreement of these two plots, however, is coincidental. While the separation of the fluid and solid branches in the q_2' diagram is due to the fact that only ordered clusters have vanishing q_2', there is a large number of possible disordered clusters that have $q_6' \approx q_6^{\mathrm{fcc}}$, in particular, perturbed icosahedral bond arrangements. These are, however, not present in the data in large numbers and thus

can be neglected.[38,73] If they occurred in significant abundance in the systems, an increase of $\langle q_6' \rangle$ would be the consequence. Values of q_6' close to q_6^{hcp} do, however, occur even in disordered systems.[38] Thus, deviations from $q_2' = 0$ arguably are a better criteria for disorder than deviations from q_6^{fcc}.

Since both fcc and hcp have $q_2' = 0$, they cannot be discerned using q_2' alone. The dense ($\phi > 0.649$) jLS packings, for example, consist of a significant fraction of hcp and fcc clusters on a disordered background. Increasing packing fraction reduces the amount of disordered configurations, and proportionally, their weight in the $\langle q_l' \rangle$ averages. Consequently, the q_2' curves tend towards $q_2' = 0$ as the ordered clusters take over a larger amount of the system, while the terminus of the q_6' curves reflects an average of q_6^{fcc} and q_6^{hcp}, weighted with the relative fraction of fcc and hcp domains. A separation of all the regimes cannot be seen in the q_4' plot (d), since q_4' takes for crystalline (fcc and hcp) phases fixed values, which are lying on a strong random background from the disordered parts of the system.

CONCLUSION

This article has clearly demonstrated that the conventional bond-orientational order parameters q_l, defined via nearest neighbor bonds, Eq. (1), are very strongly affected by the choice of neighborhood definition (cf. Fig. 2); this sensitivity is observed both in the qualitative trend and in absolute values. It was shown that for disordered systems without crystallization, q_6 strongly correlates to the average number of nearest neighbors. This effect overshadows the actual structural changes induced by the physics of the system (cf. Fig. 3). This dependence is a major drawback that needs to be taken into account when using q_l for the analysis of particulate matter, especially when comparing q_l values across different studies.

We have proposed a unique, well-defined, and robust structure metric q_l', Eq. (2), that avoids the ambiguities that come with bond network neighborhoods. Robustness of the structure metric is achieved by quantifying the geometry of the Voronoi tessellation. The MSM share the same mathematical form with the conventional bond-orientational order parameters, but the "bonds" are weighted with the associated Voronoi facet area. This guarantees, in particular, that the new Minkowski structure metrics are continuous as a function of the sphere coordinates. For hcp, fcc, and simple cubic lattices, this definition reproduces the values of the conventional q_l (cf. Table I). For super-cooled hard-sphere fluids, the MSM q_6' is very similar to the conventional q_6 with the (rarely used) $n_{\mathrm{f}} = 12$ neighborhood definition, see Fig. 2.

The morphometric neighborhood has previously been characterized using Minkowski tensors,[38,53,61] which measure the distribution of normal vectors of the Voronoi cells. The Minkowski structure metrics presented here can be interpreted as the rotational invariants of a multipole expansion of the same distribution of normal vectors; indeed, the approaches of higher-rank Minkowski tensors and Minkowski structure metrics turn out to be mathematically equivalent ways to cure the shortcomings of bond-orientational order parameters. There are further possibilities to address this problem by introducing weighting factors, see, for example, Ref. 56. Note, however, that these approaches need adjustable parameters. The caution for the use of q_6 as a sole determinant of local crystallinity expressed in Ref. 38, however, is independent of the issues addressed by this paper, and remains valid also for the Minkowski structure metric q_6'.

Thus, Minkowski tensors and structure metrics both provide a "geometrization" of the bond-orientational order for spherical particles. This suggests a strategy to generalize bond-orientational order parameters towards aspherical particles, such as ellipsoids, using generalized Voronoi tessellations and the q_l'. Even applications to non-cellular shapes with arbitrary topology are possible, albeit with altered interpretation.[63,74]

Finally, our analysis supports the more frequent use of the low-weight q_l, in particular q_2', that have been largely overlooked in the literature. q_2' carries the same information as the anisotropy index $\beta_1^{0,2}$ of Refs. 38, 53, and 61 (cf. Fig. 5). Both q_2' and $\beta_1^{0,2}$ can be used to robustly classify collective states in particulate matter according to their structural features. Furthermore, q_2' very strongly discerns between disordered configurations and such of high symmetry, such as hcp, fcc, bcc, simple cubic, and icosahedral order.

Clearly, 30 years after the seminal publication by Steinhardt *et al.*,[1] the need for quantitative local structure analysis is more evident than ever. The present paper reaffirms the validity and usefulness of the multipole expansion method. We have, however, described an amended version of the bond-orientational order parameters that not only renders this method robust and uniquely defined, but also gives a firmer interpretation of their geometric meaning.

ACKNOWLEDGMENTS

We are grateful to Tomaso Aste for the jammed LS data sets, to Shigenori Matsumoto, Tomoaki Nogawa, Takashi Shimada, and Nobuyasu Ito for the MD data, to Markus Spanner for MC data, and to the authors of Ref. 71 for publishing their Lubachevsky-Stillinger implementation. We thank Jean-Louis Barrat for his suggestion to perform this study of q_6, and to Frank Rietz for comments on the manuscript. We acknowledge support by the Deutsche Forschungsgemeinschaft (DFG) through the research group "Geometry & Physics of Spatial Random Systems" under grants SCHR 11483-1 and ME 136112-1.

[1] P. Steinhardt, D. Nelson, and M. Ronchetti, Phys. Rev. B **28**, 784 (1983).
[2] D. Nelson and B. Halperin, Phys. Rev. B **19**, 2457 (1979).
[3] P. ten Wolde, M. Ruiz-Montero, and D. Frenkel, Phys. Rev. Lett. **75**, 2714 (1995).
[4] R. Ni and M. Dijkstra, J. Chem. Phys. **134**, 034501 (2011).
[5] W.-S. Xu, Z.-Y. Sun, and L.-J. An, Eur. Phys. J. E **31**, 377 (2010).
[6] W. Lechner and C. Dellago, J. Chem. Phys. **129**, 114707 (2008).
[7] L.-C. Valdes, F. Affouard, M. Descamps, and J. Habasaki, J. Chem. Phys. **130**, 154505 (2009).
[8] T. Kawasaki and H. Tanaka, J. Phys.: Condens. Matter **22**, 232102 (2010).
[9] H. Wang and H. Gould, Phys. Rev. E **76**, 031604 (2007).
[10] Y. Wang, S. Teitel, and C. Dellago, J. Chem. Phys. **122**, 214722 (2005).
[11] A. Keys and S. Glotzer, Phys. Rev. Lett. **99**, 235503 (2007).
[12] C. Iacovella, A. Keys, M. Horsch, and S. Glotzer, Phys. Rev. E **75**, 040801 (2007).

[13]C. Chakravarty, P. G. Debenedetti, and F. H. Stillinger, J. Chem. Phys. **126**, 204508 (2007).
[14]F. Calvo and D. J. Wales, J. Chem. Phys. **131**, 134504 (2009).
[15]J. Hernández-Guzmán and E. R. Weeks, Proc. Natl. Acad. Sci. U.S.A. **106**, 15198 (2009).
[16]K. Binder and W. Kob, *Glassy Materials and Disordered Solids: An Introduction to Their Statistical Mechanics (Revised Edition)* (World Scientific, 2011).
[17]A. Ikeda and K. Miyazaki, Phys. Rev. Lett. **106**, 015701 (2011).
[18]A. V. Mokshin and J.-L. Barrat, J. Chem. Phys. **130**, 034502 (2009).
[19]H. Tanaka, T. Kawasaki, H. Shintani, and K. Watanabe, Nature Mater. **9**, 324 (2010).
[20]K. Lochmann, A. Anikeenko, A. Elsner, N. Medvedev, and D. Stoyan, Eur. Phys. J. B **53**, 67 (2006).
[21]T. Schilling, H. Schöpe, M. Oettel, G. Opletal, and I. Snook, Phys. Rev. Lett. **105**, 025701 (2010).
[22]J. S. van Duijneveldt and D. Frenkel, J. Chem. Phys. **96**, 4655 (1992).
[23]A. Wouterse and A. P. Philipse, J. Chem. Phys. **125**, 194709 (2006).
[24]N. Duff and D. Lacks, Phys. Rev. E **75**, 031501 (2007).
[25]S. Abraham and B. Bagchi, Phys. Rev. E **78**, 051501 (2008).
[26]This expression assumes that neighborhood is a symmetric concept, such that $a \in \mathrm{NN}(b)$ implies that $b \in \mathrm{NN}(a)$. This is correct for the definitions of neighborhood based on cutoff radii and on the Delaunay triangulation, but not for the definition based on a fixed number of neighbors.
[27]C. Kelchner, S. Plimpton, and J. Hamilton, Phys. Rev. B **58**, 11085 (1998).
[28]S. Edwards and D. Grinev, Physica A **302**, 162 (2001).
[29]M. Bargiel and E. M. Tory, Adv. Powder Technol. **12**, 533 (2001).
[30]P. Armstrong, C. Knieke, M. Mackovic, G. Frank, A. Hartmaier, M. Göken, and W. Peukert, Acta Mater. **57**, 3060 (2009).
[31]C. Gray and K. Gubbins, *Theory of Molecular Fluids. Volume 1: Fundamentals* (Clarendon, Oxford, 1984).
[32]E. P. Wigner, *Group Theory and its Application to the Quantum Mechanics of Atomic Spectra* (Academic Press, New York and London, 1959).
[33]Although we will not use the global bond order parameter Q_l, we define it for the sake of completeness as $Q_l = \sqrt{\frac{4\pi}{2l+1}\sum_{m=-l}^{l}\left|\frac{1}{\mathcal{N}}\sum_{a=1}^{N}\sum_{b\in\mathrm{NN}(a)}Y_{lm}(\theta_{ab},\varphi_{ab})\right|^2}$. N is the number of spherical particles and $\mathcal{N}=\sum_{a=1}^{N} n(a)$ the number of all bonds. That is, the average over all bonds is taken inside the norm. For disordered systems the sum over the Y_{lm} vanishes as $\mathcal{N}^{-1/2}$, while it remains finite for common crystalline structures.[1,58]
[34]T. Aste, M. Saadatfar, and T. Senden, Phys. Rev. E **71**, 061302 (2005).
[35]B. A. Klumov, Phys. Usp. **53**, 1053 (2011).
[36]M. Yiannourakou, I. G. Economou, and I. A. Bitsanis, J. Chem. Phys. **133**, 224901 (2010).
[37]C. L. Martin, Phys. Rev. E **77**, 031307 (2008).
[38]S. C. Kapfer, W. Mickel, K. Mecke, and G. E. Schröder-Turk, Phys. Rev. E **85**, 030301(R) (2012).
[39]Normalized bond order functions are $q_{lm}(a) := \left(\sum_{i=1}^{n(a)} Y_{lm}\right)/q_l(a)$ for particle a and the dot-product is $d_{ab} := \sum_{m=-l}^{l} q_{lm}(a)q^*_{lm}(b)$ of spheres a and b. A particle is defined as member of a solid-like cluster, if the dot-product with n_0 NN exceeds a certain threshold d_0.
[40]A. Mokshin and J.-L. Barrat, Phys. Rev. E **82**, 021505 (2010).
[41]A. Panaitescu and A. Kudrolli, Phys. Rev. E **81**, 060301(R) (2010).
[42]A. B. de Oliveira, P. A. Netz, T. Colla, and M. C. Barbosa, J. Chem. Phys. **125**, 124503 (2006).
[43]Z. Yan, S. V. Buldyrev, P. Kumar, N. Giovambattista, P. Debenedetti, and H. Stanley, Phys. Rev. E **76**, 051201 (2007).
[44]M. Wallace and B. Joós, Phys. Rev. Lett. **96**, 025501 (2006).
[45]A. Kansal, S. Torquato, and F. Stillinger, Phys. Rev. E **66**, 041109 (2002).
[46]J. R. Errington and P. G. Debenedetti, Nature (London) **409**, 318 (2001).
[47]G. Odriozola, J. Chem. Phys. **131**, 144107 (2009).
[48]R. Kurita and E. Weeks, Phys. Rev. E **82**, 011403 (2010).
[49]C. B. Barber, D. P. Dobkin, and H. Huhdanpaa, ACM Trans. Math. Softw. **22**, 469 (1996).
[50]The definition of NN via the Delaunay graph is equivalent to the definition via Voronoi neighbors: spheres share a Delaunay edge, whenever their respective Voronoi cells have a shared facet (regardless of the area of the Voronoi facet).
[51]V. Senthil Kumar and V. Kumaran, J. Chem. Phys. **124**, 204508 (2006).
[52]S. Matsumoto, T. Nogawa, T. Shimada, and N. Ito, "Heat transport in a random packing of hard spheres," e-print arXiv:1005.4295 [cond-mat.stat-mech].
[53]S. C. Kapfer, W. Mickel, F. M. Schaller, M. Spanner, C. Goll, T. Nogawa, N. Ito, K. Mecke, and G. E. Schröder-Turk, J. Stat. Mech.: Theory Exp. **2010**, P11010 (2010).
[54]Event driven MD simulations to explore the super-cooled regime use the Matsumoto algorithm from Ref. 52. In this algorithm, spheres are expanded until they touch the closest Voronoi facet or until they reach the final radius. This creates a transient polydisperse ensemble, which is relaxed by thermal motion, followed by an expansion step. This procedure is iterated until a monodisperse HS system at predefined packing fraction is obtained.
[55]L. V. Woodcock, Nature (London) **385**, 141 (1997).
[56]P. R. ten Wolde, M. J. Ruiz-Montero, and D. Frenkel, J. Chem. Phys. **104**, 9932 (1996).
[57]J. P. Troadec, A. Gervois, and L. Oger, EPL **42**, 167 (2007).
[58]M. D. Rintoul and S. Torquato, J. Chem. Phys. **105**, 9258 (1996).
[59]G. E. Schröder-Turk, W. Mickel, S. C. Kapfer, M. A. Klatt, F. M. Schaller, M. J. F. Hoffmann, N. Kleppmann, P. Armstrong, A. Inayat, D. Hug, M. Reichelsdorfer, W. Peukert, W. Schwieger, and K. Mecke, Adv. Mater. **23**, 2535 (2011).
[60]R. Schneider and W. Weil, *Stochastische Geometrie*, Teubner Skripten zur mathematischen Stochastik (B.G. Teubner, 2000).
[61]G. E. Schröder-Turk, W. Mickel, M. Schröter, G. W. Delaney, M. Saadatfar, T. J. Senden, K. Mecke, and T. Aste, Europhys. Lett. **90**, 34001 (2010).
[62]M. Doi and T. Ohta, J. Chem. Phys. **95**, 1242 (1991).
[63]G. E. Schröder-Turk, V. Trond, L. D. Campo, S. C. Kapfer, and W. Mickel, Langmuir **27**, 10475 (2011).
[64]M. E. Evans, J. Zirkelbach, G. E. Schröder-Turk, A. M. Kraynik, and K. Mecke, Phys. Rev. E **85**, 061401 (2012).
[65]S. C. Kapfer, W. Mickel, G. E. Schröder-Turk, and K. Mecke, "Spherical minkowski tensors," (unpublished).
[66]J. Jerphagnon, D. Chemla, and R. Bonneville, Adv. Phys. **27**, 609 (1978).
[67]C. Lautensack, *Random Laguerre Tessellations* (Verlag Lautensack, Bingen, Germany, 2007).
[68]H. Müller, Rend. Circ. Mat. Palermo **2**, 119 (1953).
[69]B. D. Lubachevsky and F. H. Stillinger, J. Stat. Phys. **60**, 561 (1990).
[70]In the LS algorithm,[69,71] spheres are continuously expanded with event-driven MD until the pressure exceeds a jamming threshold (jLS). The unjammed LS simulations (uLS) used here are stopped at predefined packing fractions.
[71]M. Skoge, A. Donev, F. H. Stillinger, and S. Torquato, Phys. Rev. E **74**, 041127 (2006).
[72]The anisotropy index $\beta_1^{0,2}$ is the ratio of eigenvalues of $W_1^{0,2}$ (see Eq. (4)): $\beta_1^{0,2} = \xi_{\min}/\xi_{\max}$, where $\xi_{\min} \le \xi_{\mathrm{mid}} \le \xi_{\max}$. $\beta_1^{0,2} = 1$ indicates isotropy, lower values of $\beta_1^{0,2}$ indicate anisotropy.[61]
[73]A. Anikeenko and N. Medvedev, Phys. Rev. Lett. **98**, 235504 (2007).
[74]W. Mickel, G. E. Schröder-Turk, and K. Mecke, Interface Focus **2**(5), 623 (2012).